Expanded View Figures

Figure EV1. Biochemical characterization of the hGID sub-complexes.

A–F Size-exclusion profiles of the indicated hGID sub-complexes. In the schematic representation, the catalytic core subunits composed of MAEA, RMND5a, and TWA1 is colored in blue, WDR26 in green, RanBP9 in light magenta, ARMC8 in dark red, and ZMYND19 and HBP1 in gray.

G *In vitro* pull-down assay of Strep-RanBP9 and His-WDR26 co-expressed in baculoviral *Sf9* cells, demonstrating the formation of a stable complex ($n = 2$).

H Western blot analysis of HBP1 *in vitro* ubiquitination in the presence of a hGID complex lacking the RanBP9-WDR26 module ($n = 3$).

I Size-exclusion profiles of the different endogenous hGID subunits in HeLa cells analyzed by the SEC-Explorer web platform (Heusel *et al*, 2019).

Source data are available online for this figure.

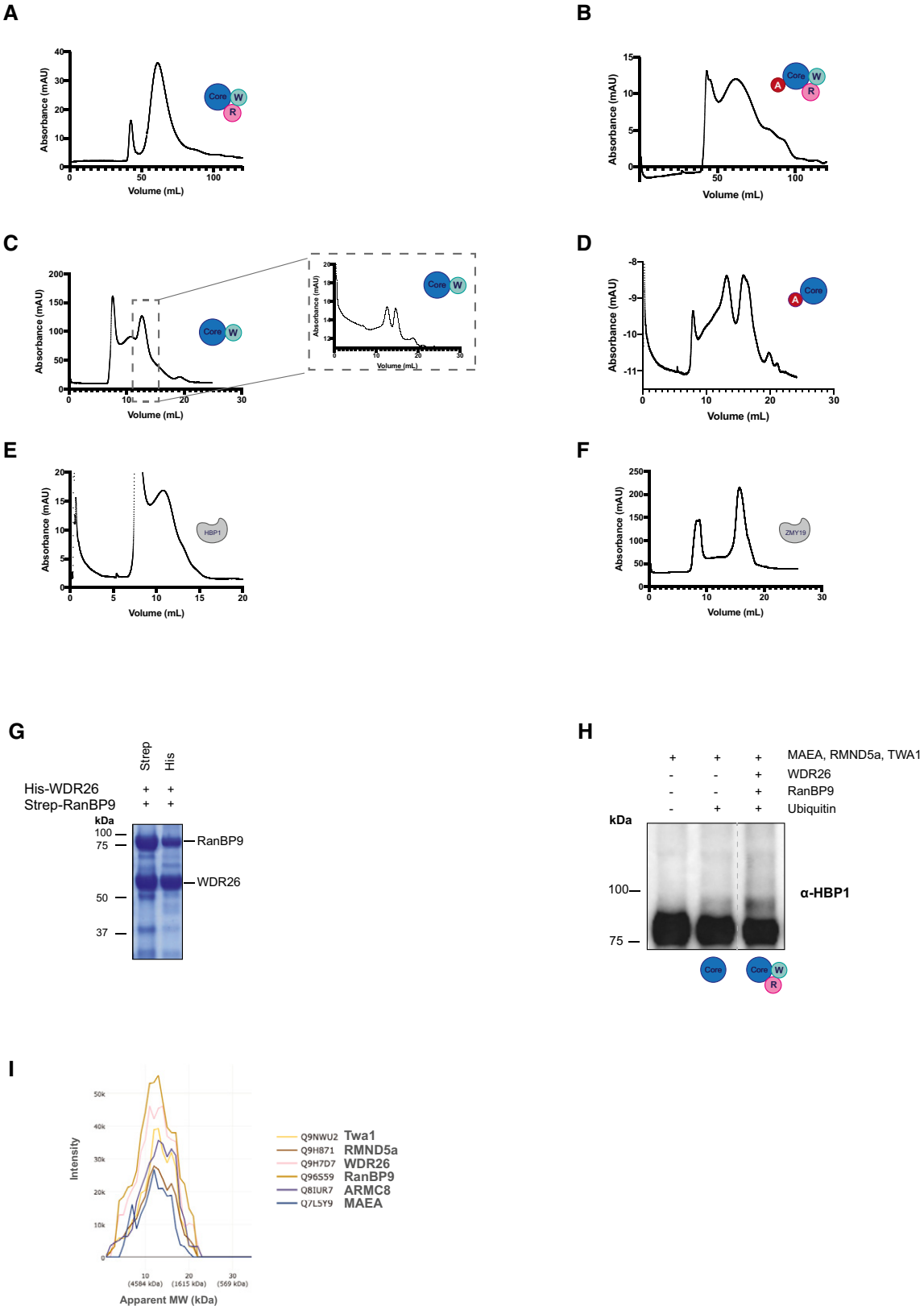
A
Absorbance (mAU)
Volume (mL)
Core
W
R
B
A
C
D
E
HBP1
F
ZMY19
G
Strep
His
His-WDR26
Strep-RanBP9
kDa
100
75
50
37
RanBP9
WDR26
H
MAEA, RMND5a, TWA1
WDR26
RanBP9
Ubiquitin
α-HBP1
I
Intensity
Apparent MW (kDa)
Q9NWU2 Twa1
Q9H871 RMND5a
Q9H7D7 WDR26
Q96S59 RanBP9
Q8IUR7 ARMC8
Q7L5Y9 MAEA

Figure EV1.

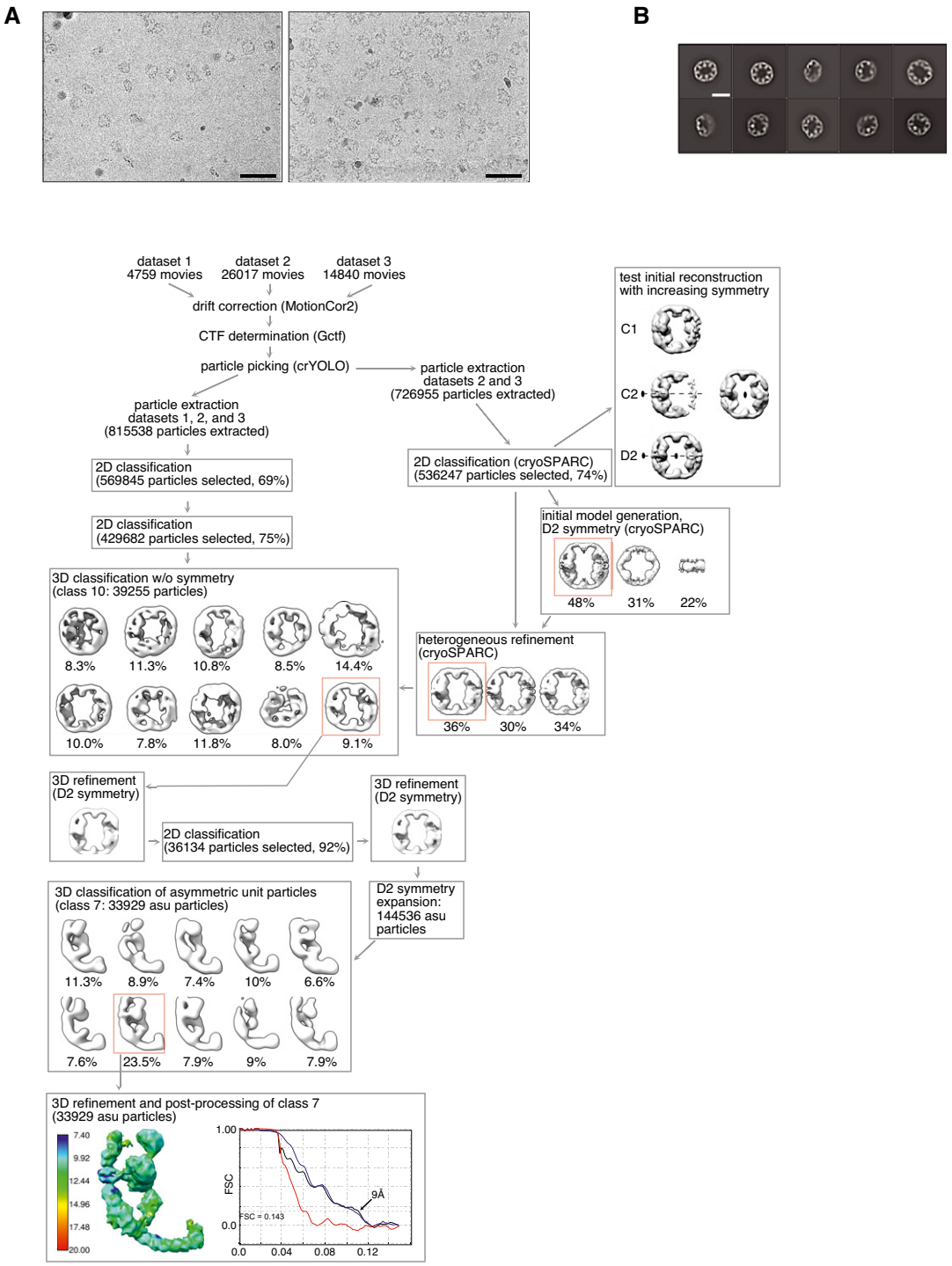

Figure EV2. Cryo-EM data analysis, classification, and refinement procedures of the 5-subunit hGID complex.

A Single particle image processing of the 5-subunit GID complex. Scale bar on Micrographs: 0.5 μm. Three datasets of the 5-subunit GID complexes were combined, and 816k particle images were extracted. An initial model was obtained with CryoSPARC. Several cycles of 2D and 3D classification were required to obtain a homogeneous set of particles for symmetry expansion in Relion. 3D classification after symmetry expansion provided a set of particles that was refined to 9 Å resolution. The local resolution map shows that the resolution of the domains extending toward the center of the ring is lower probably due to higher flexibility. The FSC plot shows the masked (blue), masked corrected (black), and phase randomized mask FSC (red).

B 2D class averages of 5-subunit hGID complex. The 10 most populated classes (of 100) are shown, ordered by occupancy. Scale bar: 20 nm.

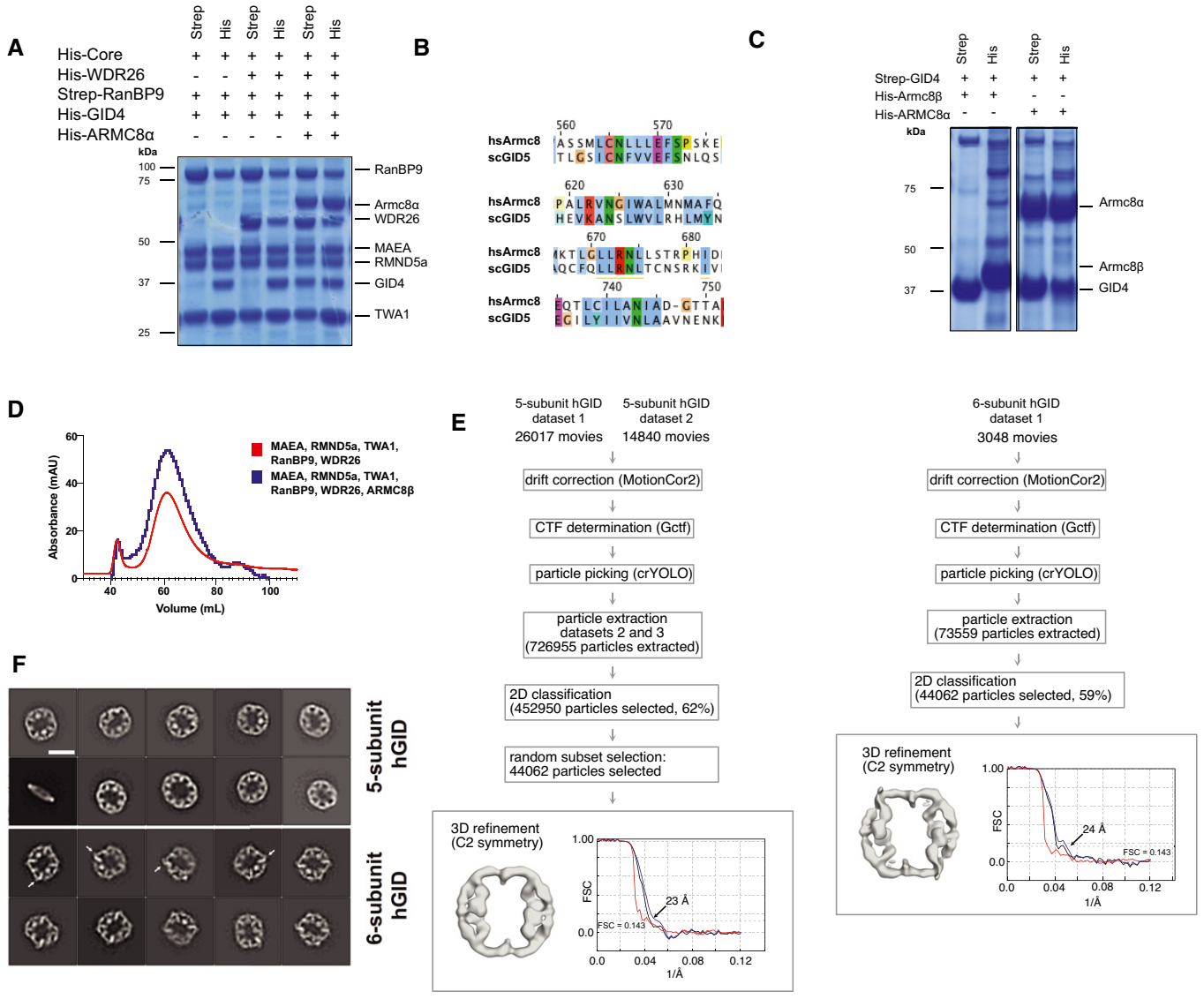

Figure EV3. Biochemical and structural characterization of the 6-subunit hGID complex and its ability to recruit GID4 subunit.

A *In vitro* pull-down assay of His-GID4 and His-ARMC8α from baculoviral *Sf9* extracts co-expressing Strep-RanBP9, His-WDR26, FLAG-MAEA, His-RMND5a, and His-TWA1. ARMC8α is required to recruit GID4 into the hGID complex (n = 3).

B Conservation between human ARMC8α and yeast Gid5 in the region required for GID4 binding using Jalview (Waterhouse *et al*, 2009) and following the Clustalx color scheme (http://www.jalview.org/help/html/colourSchemes/clustal.html).

C Baculoviral co-expression in *Sf9* cells of Strep-GID4 and His-ARMC8α or His-ARMC8β. Note that ARMC8α but not ARMC8β forms a stable complex with GID4 (n = 3).

D Comparison of the size-exclusion chromatograms from Superose 6 column (Cytiva) of the 5-subunit (RanBP9, WDR26, RMND5a, MAEA, and TWA1) and the 6-subunit (RanBP9, WDR26, RMND5a, MAEA, TWA1, and ARMC8β) hGID complexes.

E Single particle image processing scheme used to determine the difference map between 5-subunit and ARMC8β-containing 6-subunit GID complexes. The processing steps of the GID 5-subunit (left) and GID-ARMC8β 6-subunit complexes (right) were carried out with identical settings. The FSC plot shows the masked (blue), masked corrected (black), and phase randomized mask FSC (red).

F 2D class averages of the 5-subunit GID (top) and GID-ARMC8β complexes (bottom). The 10 most populated classes (of 100) are shown, ordered by occupancy. Scale bar: 20 nm. Additional density is visible in the 2D classes of the 6-subunit hGID corresponding to ARMC8β (white arrows).

Source data are available online for this figure.

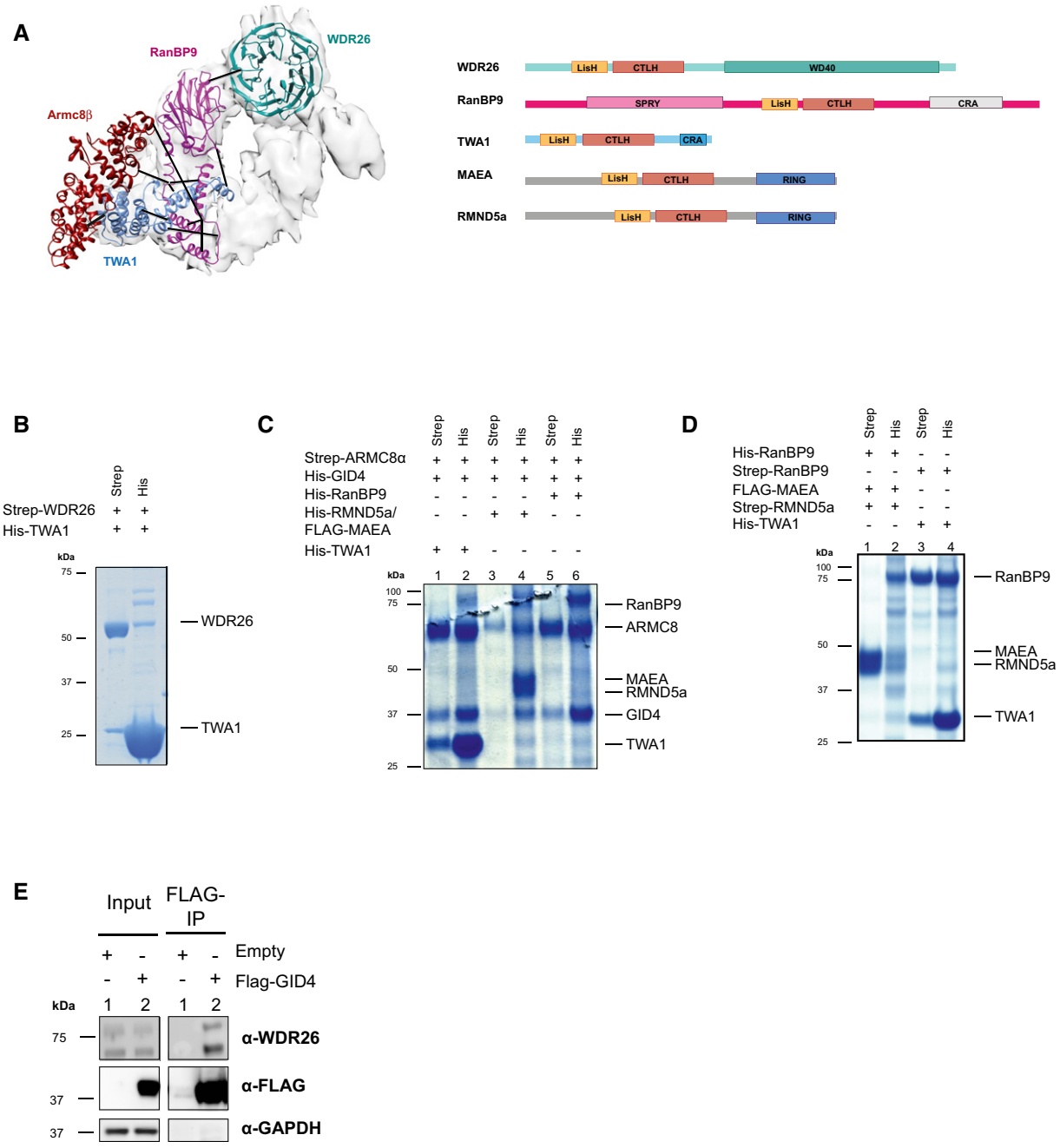

Figure EV4. Inter-subunit interactions within the hGID sub-complexes.

A The fitted homology model of RanBP9 (SPRY and LisH domain, magenta), TWA1 (blue), ARMC8β (dark red), and WD40 (dark cyan) in the 9 Å map of the 5-subunit hGID complex (gray; left panel). The observed cross-links between the different residues are indicated by black lines. Schematic architecture and domain representation of the 5 subunits (RanBP9, WDR26, RMND5a, MAEA, and TWA1) are shown to the right.

B SDS–PAGE showing *in vitro* pull-down assays using baculoviral *Sf9* co-expression of Strep-WDR26 and His-TWA1. Note that WDR26 and TWA1 directly interact ($n = 2$).

C SDS–PAGE showing *in vitro* pull-down assays using baculoviral *Sf9* co-expression of Strep-ARMC8α, which forms a complex with His-TWA1 and His-GID4 (lanes 1 and 2) but not with FLAG-MAEA and His-RMND5a (lanes 3 and 4). His-RanBP9 does not bind Strep-ARMC8α and His-GID4 (lanes 5 and 6; $n = 2$).

D His-RanBP9 does not interact with FLAG-MAEA and Strep-RMND5a (lanes 1 and 2), but Strep-RanBP9 forms a complex with His-TWA1 (lanes 3 and 4; $n = 3$).

E FLAG immunoprecipitation (FLAG IP) of extracts prepared from HEK-293T cells transiently transfected with an empty control plasmid or a plasmid overexpressing FLAG-GID4. The presence of endogenous WDR26 in the extract (input) or bound to GID4 was probed by immunoblotting. GAPDH was used as a specificity control ($n = 2$).

Source data are available online for this figure.

